multi-Risk sciEnce for resilienT commUnities undeR a changiNgclimate

Codice progetto MUR: **PE00000005** – C93C22005160002

Deliverable title: Improved models for indirect flood impacts, cascade effects and interconnections among critical infrastructures, such as energy or transport networks

Deliverable ID: 1.2.8

Due date: 01/12/2024

Submission date: 01/12

AUTHORS

Francesco Ballio (POLIMI); Daniela Molinari(POLIMI) Anna Rita Scorzini (Università dell'Aquila) Marta Bellocci (POLIMI), Panagiotis Asaridis (POLIMI), Giorgio Boni (UNIGE), Arianna Cauteruccio (UNIGE), Gabriele Moser (UNIGE), Roozbeh Rajabi (UNIGE)

1. Technical references

Project Acronym	RETURN
Project Title	multi-Risk sciEnce for resilienT commUnities undeR a changiNg climate
Project Coordinator	Domenico Calcaterra UNIVERSITA DEGLI STUDI DI NAPOLI FEDERICO II domcalca@unina.it
Project Duration	December 2022 – November 2025 (36 months)

Deliverable No.	DV#1.2.8.#
Dissemination level*	
Work Package	WP1.2 - Flood risk under environmental and climatic changes
Task	Impact Model
Lead beneficiary	POLIMI
Contributing beneficiary/ies	POLIMI, UNIVERSITA’ DELL’AQUILA, UNIVERSITA’ DI GENOVA

* PU = Public

PP = Restricted to other programme participants (including the Commission Services)

RE = Restricted to a group specified by the consortium (including the Commission Services)

CO = Confidential, only for members of the consortium (including the Commission Services)

Document history

Version	Date	Lead contributor	Description
0.1	16/11/2024	Anna Rita Scorzini (Università dell'Aquila)	First draft
0.2	21/11/2024	Daniela Molinari (POLIMI)	Critical review and proofreading
0.3	26/11/2024	Marco Borga (UNIPD)	Edits for approval
1.0	28/11/2024	Francesco Ballio (POLIMI)	Final version

2. ABSTRACT

The deliverable contains two sections: the first outlines the ISYDE/NATFIM methodology for railway and road networks, which was created with the aim of meeting the assessment and planning needs related to the Floods Directive, but with the potential for application to different sectors (e.g., for civil protection purposes), as well as for support to multi-hazard analyses.
The general methodological approach of ISYDE/NATFIM has been previously described in deliverable 1.2.3 (M12specifying nature and format of the data required for the procedure.
This deliverable provides a step-by-step detailed procedure for the implementation of the methodology into a generic informatic (territorial-based) system.
In the last paragraph recent developments of an approach for assessing flood impacts on power grids are described. Results are not yet specified as a general and usable procedure; however, they provide a significant step forward towards such aim
In the second section a supervised method for the detection of the assets at risk in case of pluvial flooding combining remote sensing and in-situ inspection is presented as well as a methodology for vulnerability assessment of the exposed assets to pluvial flooding and relative mitigation strategies.

3. Table of contents

4. Improved models for indirect flood impacts, cascade effects and interconnections among critical infrastructures

4.1 Procedure for assessing functional damage to the impacted road network

The procedure allows to identify the location of individual exposed road sections with their impact value and to aggregate data, at the scale of the census section, with the total length values of the individual road types according to their impact value.

4.1.1 . Summary of the approach

- Input: (i) hazard scenario (raster map of water depths); (ii) vector layer with linear geometry representing the road network (derived from OSM (OpenStreetMap)); (iii) polygonal vector layer representing census sections.
- Qualitative assessment of the functional damage of the flooding in terms of its impact on road traffic (due to slowdown or interruption of transit) and on the ability of the network to ensure an appropriate level of redundancy (understood as the ability to ensure that the destination can be reached), evaluated according to the type of road affected by the flooding itself.
- Representation of results at the meso-scale.

4.1.1 2. Assessment of the impact on the road network

Step 1: identification of roads/portions of roads in flooded area

- Conversion of raster map of water depths into polygonal vector layer to determine flooded area.
- Cutout of reclassified map of roads with the flooded area in vector format and identification of roads/portions of roads falling within the flooded area.

Step 2: calculation of length of flooded roads/portions of roads

- Calculation of the length of each record of the previous step output.

Step 3: attribution of water depth

- Creation of a 5 m buffer around road sections within the flooded area.
- Calculation of the average water depth h (from the raster of water depths) for each record (polygon formed by the buffer) using Zonal Statistics tools, averaging the water depths for each polygon.
- Association of the water depth found with the corresponding road section.

Step 4: assignment of the "impact" value

- Reclassification, through special computational functions, of the records of the linear theme of roads according to the "impact" of the individual road based on the combination of road type and water depths in the following matrix (resulting from the weighted average of the two matrices of transitability and redundancy):

Hazard classes	Bridges	Other (e.g. pedestrian, bicycle)	Service and/or unpaved roads	Secondary roads	Main roads	Highways	Tunnels
h = 0 m e v = 0 m/s	NULL	NULL	NULL	NULL	NULL	NULL	NULL
0 < 0.15 m< threshold	NULL	MODEST	MODEST	MODEST	MEDIUM	HIGH	HIGH
0.15 m>= threshold	NULL	MEDIUM	MEDIUM	MEDIUM	HIGH	HIGH	HIGH

In particular, all records with a value "T" (True) in the attribute "bridge" are understood as "bridges", and all records with a value "T" in the attribute "tunnel" are understood as "tunnels". For other types of roads, the new classification of the previous points applies.

Note the distinction into two hazard classes according to a threshold set at 0.15 m. This is a threshold value, derived from literature, at which the passage of vehicles of smaller dimensions is interrupted.

- Creation of a colour style that associates the "impact" values with the corresponding colours of the matrix cells in step 4. The "non-assessable" roads, i.e. those for which some information is missing, are represented in white.

Step 5: aggregation of information on the flooded portions of census sections

- Through spatial join operations, associate the information in the linear layer of step 4 with the portions of the flooded census section in which they fall and aggregate (as a total sum of lengths) the tabular information by road type and by impact.

Step 6: calculation of the unique impact indicator for roads

- Assignment of the unique impact indicator for roads (IUS) in terms of equivalent length of roads with different impacts per unit area.

Step 7: calculation of the total length of the sections exposed to the individual "impact" values

- Calculation of total lengths within the flooded area as a function of road type and impact.

4.2 Procedure for assessing functional damage to the impacted railway network and for defining exposed railway station

The procedure allows to identify the location of individual exposed railway lines with their impact value and to aggregate data, at the scale of the census section, with the total length values of the individual railway types according to their impact value. Exposed railway stations are also surveyed.

4.2.1 .Summary of the approach

- Input: (i) hazard scenario (raster map of water depths); (ii) vector layer with linear geometry representing the railway network (derived from OSM (OpenStreetMap)); (iii) point vector layer identifying the location of railway stations (derived from Italian open data (http://www.datiopen.it/it/opendata/Mappa_delle_stazioni_ferroviarie_in_Italia); (iv) polygonal vector layer representing the census sections.
- Qualitative assessment of the functional damage in terms of the impact that the slowdown or interruption of trains may have on rail traffic and on reaching the destination, depending on the importance of the railway section affected by the flooding.
- Railway stations: identification of stations in flooded areas and attribution of the "high" impact value.
- Representation of the results at the meso-scale.

4.2.2. Assessment of the impact on the railway network

Step 1a: identification of the railways/railway portions intersecting the water depth map

- Conversion of the raster map of water depths into a polygonal vector layer to determine the flooded area.
- Extraction of railway lines that fall completely within the vector flooded area.

Step 1b: identification of railways that do not intersect the water depth map but are lapped by the flooded area

- Identification of non-flooded railways/railway portions: extraction by position with "disjointed" predicate between the railway network theme and the vector flooded area.
- Creation of a 10 m buffer of the layer from the previous point.
- Overlay of the vector flooded area with the buffer defined in the previous point and selection of the buffers within the flooded area.
- Step 2a: calculation of the length of the railways/railway portions intersecting the water depth map
- Calculation of the length of each railway section identified in step 1a.

Step 2b: calculation of lengths of railways/portions of railways that do not intersect the water depths map but are lapped by the flooded area

- Elimination of railways/railway portions that do not intersect the water depths map, nor lapped by the flooded area, by using a join between the original railway theme and the polygonal buffer resulting from step 1b. Those records that do not respond correctly to the join will be deleted.
- Calculation of the length of each record of the previous step output.

Step 3a: attribution of water depth to the railways/railway portions intersecting the water depths map

- Creation of a 5 m buffer of the linear vector identified in step 1a.
- Calculation of the average water depth htratta (from the raster of water depths) for each record (polygon formed by the buffer) using Zonal Statistics tools, averaging the water depths for each polygon.
- Association of the calculated water depth with the corresponding record of the linear theme identified in step 2a.

Step 3b: attribution of water depth to railways/railway portions that do not intersect the water depths map but are lapped by the flooded area

- Calculation of the water depth hbuffer (from the raster of water depths) for each record (polygon identified at step 2b) using Zonal Statistics tools, averaging the water depths for each polygon.
- Association of the water depth calculated in the previous step with the corresponding record of the linear layer identified in step 2b.

Step 4: assignment of "impact" class

- Reclassification, through special computational functions, of the records of the two linear themes (railroads intersecting the tie map; railroads not intersecting the tie map but lapped by the flooded area) according to the "impact" of the individual railway based on the combination of type of railway line and water depth in the following matrix (resulting from the weighted average of the two matrices of transitability and relevance):

Hazard classes	Ponti	Ordinary route	TAV	Tunnels
h = 0 m e v = 0 m/s	NULL	NULL	NULL	NULL
$0 < h_{ebuffer}$ (o h_{buffer}) < 0.2 m	NULL	MODEST	MEDIUM	HIGH
$h_{ebuffer}$ (o h_{buffer}) $>= 0.2$ m	NULL	MEDIUM	HIGH	HIGH
$0 < h_{etratta}$ (o h_{tratta}) < 0.1 m	NULL	MEDIUM	HIGH	HIGH
$h_{etratta}$ (o h_{tratta}) $>= 0.1$ m	NULL	HIGH	HIGH	HIGH

In particular, all records with a value “T” (True) in the attribute “bridge” are understood as “bridges”, all records with a value “T” in the attribute “tunnel” are understood as “tunnels”, and all record with a value “TAV” in the attribute “name” are understood as “TAV” (Treno ad Alta Velocità, High Speed Train).

It can be seen that, for sections lapped by the flooded area, there is a distinction into two hazard classes depending on a fixed threshold of 0.2 m. This value is derived from the literature and it indicates the water depth at the toe of the embankment above which damage to the embankment structure and to the embankment itself can occur. For sections falling within the flooded area, a threshold of 0.1 m is used as a discriminant. This threshold is adopted to take into account the uncertainties associated with the estimates of water depth flood and to account for the situation in which, although the section intersects the flooded areas, the rails can reasonably be considered not to be submerged (in fact, for the latter, a height varying between 140-170 mm was considered).

- Association to the two linear layers of a colour style that associates the “impact” values with the corresponding colours of the matrix cells above.

Step 5: aggregation of information on the flooded portions of census sections

- Through spatial join operations, associate the information in the linear layer of step 4 with the portions of the flooded census section in which they fall and aggregate (as a total sum of lengths) the tabular information by railway type and by impact.

Step 6: calculation of the unique impact indicator for railways

- Assignment of the single unique indicator for railways (UIF) in terms of equivalent length of railways with different impacts per unit area.

Step 7: calculation of the total length of the sections exposed to the individual “impact” values

- Calculation of total lengths within the flooded area as a function of railway type and impact.

4.2.3 Impact assessment on railway stations

Step 1: identification of railway stations in flooded area

- Conversion of the raster map of the water depth into a polygonal vector layer to determine the flooded area.
- Extraction of points (stations) that fall within the flooded area.

Step 2: assignment of "impact" value

- Association of the impact value "HIGH" to all stations within the flooded area.

4.3 A conceptual framework for modelling damage to power grids

Floods can cause power outages with widespread impacts on socio-economic activities. A new framework for the assessment of flood damage to power grids enables finding the most critical assets to protect for electricity security, helping decision-makers to adopt effective risk mitigation strategies.

Power grids are critical infrastructures whose core mission is to provide secure and reliable supply of electricity. Yet, their normal operation can be significantly affected by natural hazards. Especially, floods pose a major threat of power outages that can have devastating effects on people and businesses.

For instance, thousands of people experienced power outages in the 2021 floods in Germany, Belgium and the Netherlands, remaining without access to electricity for long time periods, ranging from a few weeks to a month, before electricity supply was finally restored.

The ever-increasing dependence of modern societies and economies on electricity access for their proper functioning, combined with the potential increase in the frequency and intensity of flooding due to climate change, may expose power grids to previous unseen risks. It is therefore important to maintain the security of power supply in emergency situations triggered by natural hazards, such as floods, by taking actions to reduce the expected damage to communities and improve their climate resilience.

The need for a comprehensive damage assessment

Currently, the procedures for flood risk assessment neglect, or roughly estimate, the expected damages to power grids. Flooding of power grids can lead to three types of damage: the direct, indirect and systemic. Direct damage concerns the functional failures of network assets due to physical contact with floodwater or flood-induced riverbank erosion (i.e., physical damage). Indirect damage refers to the loss of network functionality as an indirect effect of the direct damages to the assets. Systemic damage is related to the disruption of social and economic activities that depend on power supply.

There is not yet a consolidated framework for a comprehensive analysis of flood damage to power grids, capable of capturing the full range of damaging phenomena, their cascading effects and the evaluation of their socio-economic impacts. The available methodologies face difficulties in switching between the different types of damage, hence focusing on one or maybe two specific types at a time.

Bridging the gap between flood inundation modelling and power flow modelling

Figure 1 shows a probabilistic modelling and simulation framework for the comprehensive assessment of the risk of damage to power grids in case of flooding . The framework integrates modelling tools and approaches from different disciplines. Specifically, it consists of a two-dimensional flood inundation model to generate stochastic hazard scenarios, new fragility curves to calculate the conditional failure probability of power grid assets on the hazard, a simulation-based model to analyze the power flow in the network and a socio-economic model to characterize the customer categories connected to the service areas of the grid.

The framework is an operative tool allowing to: (i) consider the magnitude and frequency of floods, (ii) evaluate the physical vulnerability of power grid assets, (iii) estimate their spatiotemporal probabilities of failure, (iv) analyze the cascading effects across power transmission and distribution networks, and (v) assess the impact of power outage on the final customers.

For the probabilistic assessment of direct, indirect and systemic damages, the framework estimates the health state (failure or operational) of the network assets exposed to the hazard, evaluate the resulting voltage profile of the power transmission and distribution networks, and assess the impact of power supply disruptions on the end-users, respectively.

A set of risk metrics is calculated for three different levels, i.e., assets, networks and people, to get the complete picture of the prevailing level of grid performance. More specifically, it calculates the number of electrical substations and cabins failed due to inundation, the amount of power not supplied to the different customer categories at steady conditions, and the number of residential, commercial, industrial and agricultural customers affected by power interruptions.

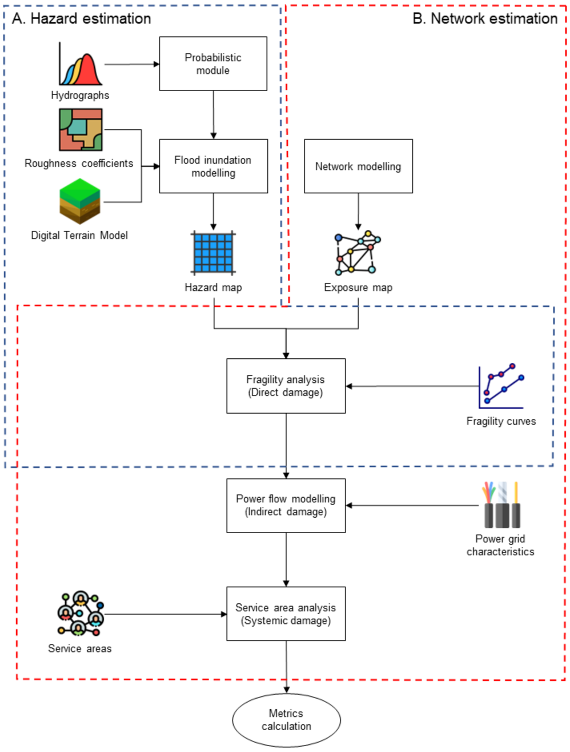

Figure 1: The flowchart of the probabilistic modelling and simulation framework.

Impact-based decision making for targeted investments

The use of the modelling and simulation tool allows the identification of the most critical network assets, whose failure would cause major power outages affecting more socio-economic activities, by performing probabilistic damage assessments associated with floods of different magnitude and frequency. The expected results can assist decision makers to formulate appropriate risk reduction strategies for increasing the resilience of power grids against more intense and frequent flood events closely linked to the changing climate.

Overall, the tool provides fundamental insights that support targeted and tailored decision-making for future investments to preserve public safety and ensure economic prosperity under climate-related emergencies.

More details on the procedure can be found in Asaridis and Molinari (2023).

4.4 Detection of exposed assets to pluvial flooding combining remote sensing techniques and in-situ inspection.

4.4.1 Introduction

The contribution of UniGe within activity A.2.8.5 aims to detect floodborne objects from aerial photos of urban areas including vehicles, trash-bin, shopping carts, and construction debris. The dataset originates from the Sampierdarena district in Genova, Italy, a region susceptible to flooding events. To accurately identify floodborne objects within the study area, advanced object detection algorithms based on deep learning techniques are employed. The insights derived from this study can be used to contribute significantly to the fields of hydrologic modeling, disaster risk reduction, and the sustainable development of urban environments.

4.4.2 Genova Sampierdarena Dataset

In this study, the Sampierdarena area in Genova has been identified within the UniGe team involved in RETURN in relation to its interest for pluvial flood studies. In Table 1, the specifications of Genova Sampierdarena dataset of aerial images that is used in current study is summarized.

Table 1: Summary of Genova Sampierdarena dataset.

Dataset	**Number of Images**	**Image Size**	**Spatial Resolution**	**Area**
Genova	814	1700 x 1100	5 cm	Sampierdarena, Genova, Italy

4.4.3 Methodology and Data Processing

The YOLO (You Only Look Once) network first introduced in CVPR 2016 (Redmon et al, 2016) uses the idea of processing the whole image in a single stage to do object detection. Its cost function comprises of localization loss for bounding box coordinates, confidence loss for object presence or absence, and classification loss for class accuracy (Terven et al, 2023). YOLOv8 is another version of YOLO released in January 2023 by Ultralytics. YOLOv8 introduced the C2f module that combines high-level features with spatial information to improve accuracy. YOLO11 is the latest version of Ultralytics YOLO series published in September 2024 (Jocher and J. Qiu, 2024) . It uses a more computationally efficient implementation of CSP bottleneck that improves spatial attention in the feature ms to concentrate on specific areas of interest and improve detection accuracy for objects with varying sizes and positions (Khanam, R. and M. Hussain, 2024). YOLOv8 and YOLO11 are published in different variants based on the number of parameters ranging from nano to extra-large. For a faster training and inference of the models, nano variants and Oriented Bounding Box (OBB) version (YOLOv8n-OBB and YOLO11n-OBB) have been used in the current study. These models are pretrained on DOTAv1 aerial images dataset.

Supervised machine learning models need well-annotated data to train with. This means that the objects of interest in the aerial photos must be labelled with their corresponding classes. The annotation process can be time-consuming and requires a lot of attention to detail, but it is essential for creating a high-quality dataset that will produce accurate results. To annotate Genova Sampierdarena dataset, the initial stage involves using pre-trained object detection models for vehicle detection on our dataset. Next step involves manual examination of the model's outputs to rectify any errors in the results and adding trash-bin class using LabelImg_OBB labeling tool (Tzutalin, 2015). This manual refinement process ensures the accuracy and reliability of the annotated dataset. Then, the model is retrained using this annotated dataset for fine-tuning. This process ensures that the models are better equipped to handle the specific characteristics of aerial imagery in our study area. Following this, all images from our dataset are passed through the fine-tuned network for the final object detection results.

4.4.4. Results and Evaluation

To evaluate object detection results we should first define Intersection over Union (IoU). IoU defined as area of overlap between predicted bounding box and ground truth bounding box over area of union. True positives are determined based on the IoU threshold value (the default value of 0.6 is used in our study).

The results based on confusion matrices are summarized in

Table 2 for the YOLOv8n-OBB and YOLO11n-OBB models trained partially on Genova dataset. Confusion matrix summarizes true positives, false positives, false negatives, and true negatives for all classes. In the training phase, at this point, we only used 3% of image patches of size 1700x1100 pixels. *Table 3* provides a detailed comparison of the models in terms of standard object detection metrics. Precision measures the accuracy of positive predictions. Recall measures the percentage of true objects in the image that the model successfully detects. Mean Average Precision (mAP) value calculated at IoU threshold of 0.5 over all classes. The last metric in this table is mAP50-95 (mAP at IoU threshold of 0.5 to 0.95) that calculates the average of mAP for different values of IoU threshold ranging from 0.5 to 0.95 in steps of 0.05. This metric gives a more complete measure of model performance in different levels of object detection difficulty.

Table 2. Normalized confusion matrix for YOLOv8n-OBB, and YOLO11n-OBB models on Genova dataset.

Model	YOLOv8n-OBB				YOLOv11n-OBB			
		TRUE				**TRUE**		
	PRED	VEH	TB	BG	**PRED**	VEH	TB	BG
Train	VEH	0.98	0.01	0.57	VEH	0.98	0	0.42
	TB	0	0.88	0.43	TB	0	0.88	0.58
	BG	0.02	0.11	0	BG	0.02	0.12	0
Validation	VEH	0.97	0	0.79	VEH	0.95	0.07	100
	TB	0	0.8	0.21	TB	0	0.6	0
	BG	0.03	0.2	0	BG	0.05	0.33	0
Test	VEH	0.92	0	0.56	VEH	0.95	0	0.82
	TB	0.01	0.62	0.44	TB	0	0.69	0.18
	BG	0.08	0.37	0	BG	0.05	0.31	0

Table 3. Comparison of results of the YOLOv8n-OBB and YOLO11n-OBB models on the Genova dataset with 5cm spatial resolution.

Model name	Split	Images	Instances	Precision	Recall	mAP 50	mAP 50-95
YOLOv11n-OBB	Train	30	899	0.94	0.93	0.94	0.79
	Val	5	179	0.92	0.87	0.92	0.76
	Test	5	172	0.97	0.81	0.85	0.75
YOLOv8n-OBB	Train	30	899	0.94	0.92	0.94	0.77
	Val	5	179	0.93	0.88	0.93	0.77
	Test	5	172	0.75	0.81	0.77	0.67

The sample results presented in Figure 2 showcase the detection capabilities of the employed models on the Genova dataset. Considering the results of both models, the trained networks are effective in the detection of vehicle (accuracy of 95%), but the performance for the trash-bin (accuracy of 69%) is still needs to be improved. The major reason is that there is no class of trash-bin in the pre-trained model and the models generally need more training samples to learn this class.

	YOLOv8n-OBB	YOLOv11n-OBB
Train		
Val		
Test		

Figure 2. Sample results of YOLOv8n-OBB and YOLO11n-OBB models for Genova dataset.

4.5 Vulnerability assessment of assets exposed to pluvial flooding and development of mitigation strategies

4.5.1 Introduction

In this section the role of permeable pavements (PPs) in the mitigation of pluvial flooding is modelled using the HEC-RAS software to simulate different rainfall intensity and stormwater inlet efficiency scenarios. The proposed approach was applied to the proof of concept, already introduced in the previous DV 2.1 of WP 2, located in the town of Genoa (Italy) in the Sampierdarena district. Laboratory tests were carried out to assess the hydrological performance of a permeable pavement already used, by the Municipality of Genova, for the reconversion project of a former military area.

Finanziato dall'Unione europea
NextGenerationEU
Ministero dell'Università e della Ricerca
Italiadomani
PIANO NAZIONALE DI RIPRESA E RESILIENZA

4.5.2 Mitigation strategies for pluvial flooding

The response hydrographs of a continuous resin gravel PP were obtained from tests carried out on a laboratory testbed for different rainfall intensity and slope. The results were interpreted using a mathematical model based on the analogy of the step response of the first- and second-order dynamical systems (Cauteruccio et al., 2024). Synthetic performance indices and their functional dependencies were obtained. The response model was calibrated using test results and then validated against further tests that had not been used for calibration (see Figure1).

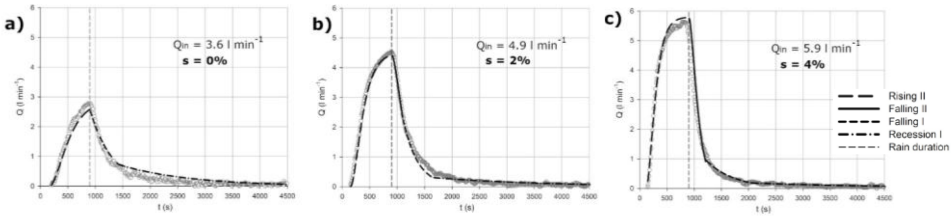

Figure 3 Hydrological response of the resin gravel PP at different slope and inflow rates: validation of the mathematical formulation used (lines) and calibrated based on laboratory results (circles). Validation tests were not used for calibration. [Source: Cauteruccio et al., 2024].

The hydraulic response of PPs was introduced into a flood simulation model (developed using the HEC-RAS software), to replace impervious sidewalks and traffic island pavements. As this cannot be modelled directly in HEC-RAS, an external code was used. Precipitation over such permeable areas (clustered in suitable blocks) was first excluded from the calculation to ensure that they do not directly contribute to the runoff. Both the sub-surface flow and infiltration were computed externally for each block under any given rainfall scenario. The sub-surface flow that contributes to the street runoff was then introduced into the HEC-RAS model in the form of an inflow hydrograph (consistent with the forcing rainfall scenario) and was positioned at the block boundaries. The detention effect and runoff reduction achieved by the introduction of the permeable pavements were obtained as a function of an appropriate deep infiltration coefficient. Stormwater inlets were modelled as pumping stations, controlled by a set of operating rules that reproduce their head-flow relationship as a function of the water surface elevation at the inlet location. The operating conditions adopted for the inlets (free, clogged or partially clogged) are those observed during a dedicated field survey.

Rainfall scenarios include synthetic events associated with different return periods. Different values of the infiltration coefficient were tested for the blocks, corresponding to different soil types and conditions below the permeable pavement (from impervious to highly permeable). Flood maps produced under different scenarios were compared (see Chinchella et al., 2024) to assess the role of inlet conditions and the flood risk reduction achieved by using a specific PP whose hydrological response is known as a function of the terrain slope and rainfall intensity.

The results show that both the extension of the flooded area and the maximum water depth reached during the event are reduced after the introduction of PPs. The temporal evolution of the flooding event is also affected. The detention effect of PPs is highlighted by the time shift of the cumulative flood water volume, while the retention is provided by the improved infiltration capacity. Finally, the simulations show that, even assuming a limited soil infiltration capacity, the implementation of PPs provides significant mitigation of pluvial flooding events.

4.5.3 Synergies with other projects

The survey of inlets, data collection and the development of the flood modelling code were carried out within the project RUN – "Urban Resilience: Now-casting of the risk of flooding with IoT sensors and Open Data", funded within the ROP-ERDF (Regional Operational Programme of the European Regional Development Fund). The hydraulic performance of permeable pavements was obtained from laboratory tests carried out within the Urban NAture LABs (UNALAB) project, funded under the "HORIZON 2020" programme, Smart and sustainable Cities - SCC-02-2016-2017. This work is published in Cauteruccio et al. (2024) and Chinchella et al. (2024)

5. Conclusions

In the first part of this deliverable, procedures for the calculation of indirect damages / impacts to transport networks are identified and described step by step; they can be implemented in the "Digital Twin", as a valuable component of the informatic ecosystem developed within VS1 as an interoperable tool among the different spokes of the Return project.

Model for assessing impact to other networks (electricity, gas, data, water,) still require significant research and development. In this report we described a state of the art approach for assessing impacts to power grid, to be developed into an operational procedure.

A second part presents the state-of-the-art of object detection models for floodborne object detection. Specifically vehicles and trash-bins are of interest in our study. The experiments are conducted for the case study of Genova Sampierdarena on a high-resolution aerial images dataset. We retrained models using a small set of images to adjust them for this study area. According to the obtained results, the performance for vehicle detection is highly satisfactory. In the case of the detection of trash bins, the performance is quite good already, especially considering the very small number of instances of this type of objects in the training set. More trash-bin samples would be necessary to further improve performance.

The last part presents the effects of mitigation strategies of pluvial flooding such as permeable pavements (PP). The results show that both the extension of the flooded area and the maximum water depth reached during the event are reduced after the introduction of PPs. The temporal evolution of the flooding event is also affected.

6. References

Asaridis, P. and Molinari, D.: A conceptual model for the estimation of flood damage to power grids, Adv. Geosci., 61, 1–21, https://doi.org/10.5194/adgeo-61-1-2023, 2023.

Cauteruccio, A., Arata, L., Parodi, M., Chinchella, E., and Lanza, L.G. (2024). Laboratory testing and modelling of the hydrological performance of a resin gravel permeable pavement. Hydrological Sciences Journal, (conditionally accepted).

Chinchella, E., Cauteruccio A., and Lanza, L.G. (2024). Mitigation of pluvial flooding using permeable pavements. CSDU International Conference on Challenges and perspectives in urban water management systems. University of Calabria, December 2-3, 2024, (submitted).

Jocher, G. and J. Qiu, Ultralytics YOLO11, 2024. [Online]. Available: https://github.com/ultralytics/ultralyticsì

Khanam, R. and M. Hussain, YOLOv11: An Overview of the Key Architectural Enhancements, arXiv preprint arXiv:2410.17725, 2024.

Redmon, J., S. Divvala, R. Girshick, and A. Farhadi: You Only Look Once: Unified, Real-Time Object Detection, in Proceedings of the IEEE Conference on Computer Vision and Pattern Recognition (CVPR), Jun. 2016.

Terven,J., D.-M. Córdova-Esparza, and J.-A. Romero-González, A Comprehensive Review of YOLO Architectures in Computer Vision: From YOLOv1 to YOLOv8 and YOLO-NAS, Mach Learn Knowl Extr, vol. 5, no. 4, pp. 1680–1716, 2023, doi: 10.3390/make5040083

Tzutalin, D. LabelImg, Github, 2015, Accessed: Nov. 04, 2024. [Online]. Available: https://github.com/heshameraqi/labelImg_OBB